Int J. Solids Structures, 1977, Vol. 13, pp. 479–492. Pergamon Press. Printed in Great Britain

STATE OF STRESS AT THE VERTEX OF A QUARTER-INFINITE CRACK IN A HALF-SPACE

J. P. BENTHEM
Laboratory of Engineering Mechanics, Delft University of Technology, Mekelweg 2, Delft, The Netherlands

(*Received* 11 *May* 1976; *revised* 19 *October* 1976)

Abstract—Spherical coordinates are r, θ, ϕ. The half-space extends in $\theta < \pi/2$. The crack occurs along $\phi = 0$. The region to be investigated is the solid space-triangle (or cone) between the three planes $\theta = \pi/2$, $\phi = +0$ and $\phi = 2\pi - 0$, which planes are to be taken stress-free.

In this space-angle a state of stress is considered in terms of the cartesian stress components

$$\sigma_{xx} = r^{\lambda} f_{xx}(\lambda, \theta, \phi); \quad \sigma_{xy} = r^{\lambda} f_{xy}(\lambda, \theta, \phi); \text{ etc.}$$

Possible values λ are determined from a characteristic (or eigenvalue) equation, expressing the condition that a determinant of infinite order is equal to zero. The root of λ which gives the most serious state of stress in the vertex region (the region $r \to 0$) is the root closest to the limiting value $Re\,\lambda > -\frac{3}{2}$. Knowledge of this state of stress, or at least of this value of λ is essential in the determination of the three-dimensional state of stress around a crack in a plate for distances of order of the plate thickenss.

Along the front of the quarter-infinite crack (z-axis) the so called stress-intensity factor behaves like $z^{\lambda+\frac{1}{2}}$ ($z \to 0$) and thus tends to zero, respectively to infinity, accordingly to $Re\,\lambda$ being $> -\frac{1}{2}$ or $< -\frac{1}{2}$. But in the region $z \to 0$ the notion stress-intensity factor loses its meaning. The required state of stress passes into the well-known state of plane strain around a crack tip if Poisson's ratio (ν) tends to zero. The computed state of stress for the incompressible medium ($\nu = \frac{1}{2}$) is confirmed by experiment.

1. INTRODUCTION

The quarter-infinite crack in a half-space is shown in Fig. 1. Cartesian coordinates are x, y, z, spherical coordinates are r, θ, ϕ.

$$\begin{aligned} x &= r \sin\theta \cos\phi \\ y &= r \sin\theta \sin\phi \\ z &= r \cos\theta. \end{aligned} \tag{1.1}$$

The half-space extends in $z > 0$. The crack occurs in the quarter-plane $y = 0, x > 0, z > 0$. Our purpose will be to determine a state of stress in the half-space around the crack in the form

$$\begin{aligned} \sigma_{xx} &= r^{\lambda} f_{xx}(\lambda, \theta, \phi) \\ \sigma_{xy} &= r^{\lambda} f_{xy}(\lambda, \theta, \phi) \\ &\text{etc.,} \end{aligned} \tag{1.2}$$

which leaves the crack surfaces and the plane $z = 0$ stress free. We shall arrive at a transcendental equation for λ and only values of $Re\,\lambda > -\frac{3}{2}$ are allowable, in order that the strain energy in the vertex region (the region $r \to 0$) remains finite (integrable). We shall determine in the first place the gravest (predominant, most serious) exponent λ, i.e. the exponent closest to the limiting value $> -\frac{3}{2}$ for different Poisson's ratio's. For this exponent we shall give the three non-zero stresses and the three displacement components of the surface $z = 0$ of the half-space. Further we shall restrict ourselves to the determination of the six exponents closest to the gravest one.

Knowledge of the gravest state of stress, or at least of the gravest exponent λ, seems to be essential in the determination of the three-dimensional state of stress around a crack tip in a plate for distances of the order of the plate thickness, whatever method for this determination may be tried. Sih[1] recognises that this exponent was still unknown and he writes "In this connection the solution obtained from a numerical analysis (without the knowledge of this exponent) is always in question".

Many more particulars about the present investigation are given in Ref. [2].

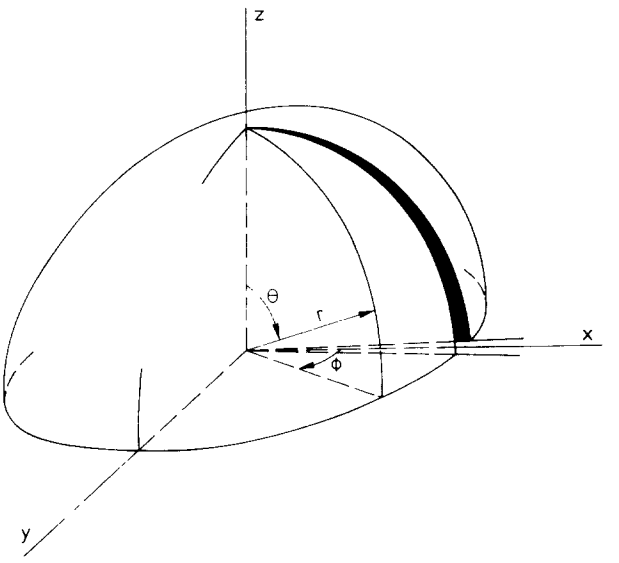

Fig. 1. The half-space $z > 0$ with the quarter-infinite crack $y = 0$, $x > 0$, $z > 0$. Cartesian coordinates x, y, z. Spherical coordinates r, θ, ϕ.

2. TWO- AND THREE-DIMENSIONAL EIGENVALUE PROBLEMS

Williams[3] determined two-dimensional stress singularities resulting from various boundary conditions in angular corners (wedges) of plates in extension.

Such a two-dimensional analysis of a wedge may start by seeking a solution for Airy's stress function $\psi(r, \phi)$ in the form

$$\psi = r^{\lambda+2} f(\lambda, \phi) \tag{2.1}$$

for

$$\Delta\Delta\psi = 0,$$

where r and ϕ are polar coordinates. Stresses behave like r^{λ}. From the boundary conditions, for example one wedge-boundary stress-free, one wedge-boundary with zero-displacements, a transcendental (eigenvalue) equation for λ is established. Only values $Re\,\lambda > -1$ are allowed, otherwise the strain energy in the vertex region would be infinite (non integrable). In the very neighbourhood of the vertex, the state of stress (2.1) belonging to the root (or the two conjugate-complex roots) closest to -1 will overwhelm the state of stress of the other roots.

For the two-dimensional wedge-problems, eigenvalue equations have always an infinite enumerable number of roots for the exponent λ with real part greater than -1, as well as smaller than -1. It may be proved (by means of Mellin-transform technique) that the states of stress, belonging to the roots with real part greater than -1 can describe the state of stress in the vertex region of a wedge.

The eigenvalue equation for the wedge in plane strain with both boundaries stress free becomes (for wedge angle α)

$$[\sin\{(\lambda+1)\alpha\}]^2 - (\lambda+1)^2 \sin^2\alpha = 0. \tag{2.2}$$

For the vertex region around a crack tip (wedge of wedge angle $\alpha = 2\pi$) this equation is

$$\{\sin 2\pi(\lambda+1)\}^2 = 0. \tag{2.3}$$

The eigenvalues λ (greater than -1) are $-\frac{1}{2}$, 0, $\frac{1}{2}$, 1, $\frac{3}{2}$, ... and indeed the well-known root-singularity ($\lambda = -\frac{1}{2}$) presents itself.

The state of plane strain in the free-free wedge of angle 2π cannot be present around a crack front which is normal to the boundary of a half-space, unless Poisson's ratio (ν) is zero. In the neighbourhood of the origin or vertex (Fig. 1) the state of stress is essentially three-dimensional accordingly (1.2) and a three-dimensional eigenvalue-problem has to be solved. It was necessary to solve the eigenvalue λ from a determinantal equation, where the determinant was of infinite order.

Since it was evident that for Poisson's ratio $\nu = 0$ a solution for λ was $-\frac{1}{2}$, it was tentatively assumed that $\lambda = -\frac{1}{2}$ was also the gravest exponent† and that for other Poisson's ratios, the gravest exponent would also be real. Therefore the search for exponents λ was primarily only for real roots and indeed the gravest exponent proved to be real, as well as the six next gravest ones (four of them are trivial).

For regions more or less like the region of the quarter-infinite crack in the half-space, Fig. 1, Bažant[4] determined the gravest exponent and the corresponding states of stress with a finite-element method. Obviously the author of [4] had to confine himself to problems which could be reduced to potential problems, for example the problem of a wedge-shaped smooth rigid stamp acting on a half-space.

The following theorems are valid for elastic regions in the form of infinite cones: (1) If an infinite conical region is loaded by stresses which behave along the generators like r^λ and if displacements are prescribed which are zero or behave like $r^{\lambda+1}$, then there is generally a solution for the interior stresses of the form

$$\begin{aligned} &\sigma_{xx} = r^\lambda f_{xx}(\lambda, \theta, \phi) \\ &\sigma_{xy} = r^\lambda f_{xy}(\lambda, \theta, \phi) \\ &\text{etc.} \end{aligned} \tag{2.4}$$

with the exception of an infinite enumerable set of values for λ. (2) For every value of λ of the infinite enumerable set meant under (1), there exists a state of stress (2.4) wherefor the prescribed stresses and displacements from (1) are zero. Such states of stress are called the eigenfunctions of the cone in question. (3) The infinite enumerable states of stress (with $Re\,\lambda > -\frac{3}{2}$) meant in (2), are able to describe the state of stress in the vertex region.

The proofs of these theorems are laborious, but in principle they may be performed along the same lines as for two-dimensional wedges (again by means of Mellin-transform technique).

3. THE BOUSSINESQ-PAPKOVICH-NEUBER STRESS-FUNCTIONS

Bousinesq created 7 basic solutions of the Navier–Cauchy equations‡ with the aid of harmonic functions. If $\psi_1 \ldots \psi_7$ are harmonic functions, these solutions are (u, v, w are the cartesian displacement components)

$$\begin{aligned} u &= 0 \\ v &= \partial\psi_1/\partial z \\ w &= -\partial\psi_1/\partial y \end{aligned} \qquad \text{(sol. 1)}$$

$$\begin{aligned} u &= -\partial\psi_2/\partial z \\ v &= 0 \\ w &= \partial\psi_2/\partial x \end{aligned} \qquad \text{(sol. 2)}$$

$$\begin{aligned} u &= \partial\psi_3/\partial y \\ v &= -\partial\psi_3/\partial x \end{aligned} \qquad \text{(sol. 3)}$$

†I.e. there is no other root in the region $-\frac{3}{2} < Re\,\lambda < -\frac{1}{2}$. The condition $Re\,\lambda > -\frac{3}{2}$ follows from the requirement that the strain-energy should remain finite in the vertex region. In order that the existence and uniqueness theorems for finite elastic bodies hold, this is the proper requirement and not as is sometimes stated: the displacements should remain finite. Latter requirement would lead to $Re\,\lambda \geq -1$. Only in two-dimensional (wedge) problems both requirements lead practically to the same conditions, viz. $Re\,\lambda > -1$ and $Re\,\lambda \geq -1$ respectively. In the present problem no roots λ are found in the region $-\frac{3}{2} < Re\,\lambda < -1$. This means one has not to face unbounded displacements at the vertex. Probably neither in any other three-dimensional cone-problem of elasticity theory.

‡These equations are valid for $-1 < \nu < \frac{1}{2}$, the basic solutions apply also to the case $\nu = \frac{1}{2}$.

$$w = 0$$

$$u = \partial\psi_4/\partial x$$
$$v = \partial\psi_4/\partial y \tag{sol. 4}$$
$$w = \partial\psi_4/\partial z$$

$$u = (-3+4\nu)\psi_5 + x\partial\psi_5/\partial x$$
$$v = x\partial\psi_5/\partial y \tag{sol. 5}$$
$$w = x\partial\psi_5/\partial z$$

$$u = y\partial\psi_6/\partial x$$
$$v = (-3+4\nu)\psi_6 + y\partial\psi_6/\partial y \tag{sol. 6}$$
$$w = y\partial\psi_6/\partial z$$

$$u = z\partial\psi_7/\partial x$$
$$v = z\partial\psi_7/\partial y \tag{sol. 7}$$
$$w = (-3+4\nu)\psi_7 + z\partial\psi_7/\partial z.$$

The functions $\psi_4, \ldots \psi_7$ are known today as the Papkovich–Neuber stress-functions. It is well established that every solution of the Navier–Cauchy equations may be considered to be a sum of the 4 basic solutions 4 . . . 7 (and often only a sum of 3 of them, for example in a convex region).

We give the dependencies of the basic solutions 1 . . . 7 the following form, which seems not to have been published before (ψ is an harmonic function†)

$$\text{sol. 1}\left(\psi_1 = \frac{\partial\psi}{\partial x}\right) + \text{sol. 2}\left(\psi_2 = \frac{\partial\psi}{\partial y}\right) + \text{sol. 3}\left(\psi_3 = \frac{\partial\psi}{\partial z}\right) = 0, \tag{3.1}$$

$$\text{sol. 2}\left(\psi_2 = \frac{\partial\psi}{\partial z}\right) - \text{sol. 3}\left(\psi_3 = \frac{\partial\psi}{\partial y}\right) = \text{sol. 4}\left(\psi_4 = \frac{\partial\psi}{\partial x}\right), \tag{3.2}$$

$$\text{sol. 6}\left(\psi_6 = \frac{\partial\psi}{\partial z}\right) - \text{sol. 7}\left(\psi_7 = \frac{\partial\psi}{\partial y}\right) = \text{sol. 1}\{\psi_1 = (-4+4\nu)\psi\} + \text{sol. 4}\left(\psi_4 = y\frac{\partial\psi}{\partial z} - z\frac{\partial\psi}{\partial y}\right), \tag{3.3}$$

$$\text{sol. 5}\left(\psi_5 = \frac{\partial\psi}{\partial x}\right) + \text{sol. 6}\left(\psi_6 = \frac{\partial\psi}{\partial y}\right) + \text{sol. 7}\left(\psi_7 = \frac{\partial\psi}{\partial z}\right)$$
$$= \text{sol. 4}\left\{\psi_4 = (-4+4\nu)\psi + x\frac{\partial\psi}{\partial x} + y\frac{\partial\psi}{\partial y} + z\frac{\partial\psi}{\partial z}\right\} \tag{3.4}$$

and of course some cyclic interchangements.

4. A SEPARATION OF VARIABLES TECHNIQUE

Self-equilibrating states of stress (the eigenfunctions) subjected to boundary conditions which leave the half-space surface stress-free ($\sigma_{zx} = \sigma_{zy} = \sigma_{zz} = 0$) and the crack surfaces stress-free ($\sigma_{yx} = \sigma_{yy} = \sigma_{yz} = 0$) will be sought.

In this procedure we rely upon the seven basic solutions 1 . . . 7 of the Navier–Cauchy equations, avoiding of course their mutual dependencies (3.1) . . . (3.4).

Seven functions $\psi_1 \ldots \psi_7$ separated into the variables of the spherical coordinates are considered.

$$\psi_1 = r^{\lambda+2} \exp i\mu\phi P^{\mu}_{\lambda+2}(\cos\theta), \psi_2 = \ldots, \ldots, \psi_7 = \ldots, \tag{4.1}$$

where $P^{\mu}_{\lambda+2}(\cos\theta)$ is an associated Legendre function of the first kind and μ and λ may have any complex value. The differentiation formulas for the harmonics such as (4.1) are‡

†Then also $\partial\psi/\partial x$ and the other arguments are harmonic.

‡$(a)_n$ is Pochhammer's Symbol, $n = 0, 1, 2, \ldots, (a)_0 = 1, (a)_n = a(a+1)(a+2)\ldots(a+n-1)$, ($n$ factors), note $(a)_1 = a$.

$$\frac{\partial\psi}{\partial x} = \tfrac{1}{2}(-\lambda-\mu-2)_0 r^{\lambda+1}\exp i(\mu+1)\phi P_{\lambda+1}^{\mu+1}(\cos\theta)$$
$$-\tfrac{1}{2}(-\lambda-\mu-2)_2 r^{\lambda+1}\exp i(\mu-1)\phi P_{\lambda+1}^{\mu-1}(\cos\theta)$$
$$\frac{\partial\psi}{\partial y} = -\tfrac{1}{2}i(-\lambda-\mu-2)_0 r^{\lambda+1}\exp i(\mu+1)\phi P_{\lambda+1}^{\mu+1}(\cos\theta) \tag{4.2}$$
$$-\tfrac{1}{2}i(-\lambda-\mu-2)_2 r^{\lambda+1}\exp i(\mu-1)\phi P_{\lambda+1}^{\mu-1}(\cos\theta)$$
$$\frac{\partial\psi}{\partial z} = -(-\lambda-\mu-2)_1 r^{\lambda+1}\exp i\mu\phi P_{\lambda+1}^{\mu}(\cos\theta).$$

Starting from the seven basic solutions (4.1), the differentiation formulas (4.2) allow to compute their displacements, strains and stresses.

We now construct from the seven basic solutions, three other solutions, sol. A, sol. B and sol. C which already satisfy the boundary conditions along the crack surfaces, but not yet along the half-space surface. *However, in the present investigation we limit ourselves to stress-systems which are symmetrical with respect to the plane* $\phi = \pi$. These solutions are (G is the shear modulus)

$$\text{sol. } A = \text{sol. } 2\,(\psi_2 = \psi_A)$$
$$\psi_A = r^{\lambda+2}\cos\mu\phi P_{\lambda+2}^{\mu}(\cos\theta)/G$$
$$\mu = 0, -1, -2, \ldots$$
$$\text{sol. } B = \text{sol. } 1\,\{\psi_1 = (1-\nu)\psi_B\} + \text{sol. } 6\,(\psi_6 = \tfrac{1}{2}\partial\psi_B/\partial z)$$
$$\psi_B = r^{\lambda+2}\sin\mu\phi P_{\lambda+2}^{\mu}(\cos\theta)/G \tag{4.3}$$
$$\mu = -1, -2, -3, \ldots$$
$$\text{sol. } C = \text{sol. } 4\,\{\psi_4 = (\tfrac{1}{2}-\nu)\psi_C\} + \text{sol. } 6\,(\psi_6 = \tfrac{1}{2}\partial\psi_C/\partial y)$$
$$\psi_C = r^{\lambda+2}\sin\mu\phi P_{\lambda+2}^{\mu}(\cos\theta)/G$$
$$\mu = -\tfrac{3}{2}, -\tfrac{5}{2}, -\tfrac{7}{2}, \ldots.$$

Some of their stresses are given in Table 1, 2 and 3.†

In the solutions A, B and C the value of λ occuring in the exponent of the radial part (for the stresses r^λ) is still arbitrary, with the only restriction $Re\,\lambda > -\frac{3}{2}$.

The chosen μ values are such that the stresses σ_{yx}, σ_{yy}, σ_{yz} are indeed zero at both crack-surfaces. They were subjected to the restriction that along the crackfront (along the z-axis) the strain energy must remain finite, this means that along the crackfront the behaviour

$$\theta^\gamma$$

of the stresses must be such that $\gamma > -1$. One could try other μ values or the use of associated Legendre functions of the second kind $Q_\lambda^\mu(\cos\theta)$ such that also the crack surfaces are stress-free. Then however, one either has $\gamma = -1, -\frac{3}{2}, -2, -\frac{5}{2}, \ldots$, or one arrives at solutions differing only a constant factor from those already taken into account (which have $\gamma = -\frac{1}{2}, 0, \frac{1}{2}, 1, \frac{3}{2}, \ldots$).

For the further development we have now at our disposal three infinite sets of enumerable solutions which are, at least for arbitrary values of λ, linearly independent. It was very carefully investigated whether there may exist still other independent solutions, separated into variables θ and ϕ, obeying the crack-conditions, but no others exist (for arbitrary values of λ and $-1 < \nu < \frac{1}{2}$). Apparently all possibilities to create such solutions by the separation of variables technique in θ and ϕ from the basic solutions 1...7 have been exhausted.

For the incompressible medium ($\nu = \frac{1}{2}$) there is a further independent solution, because one

†For the other stresses and the displacements as well as stresses and displacements of solutions created in Section 6, see Ref. [2].

Table 1. Solution A, $\mu = 0, -1, -2, -3, \ldots$

$$\sigma_{yx} = \tfrac{1}{2}(-\lambda-\mu-2)_1 r^\lambda \sin(\mu+1)\phi P_\lambda^{\mu+1}(\cos\theta) + \tfrac{1}{2}(-\lambda-\mu-2)_3 r^\lambda \sin(\mu-1)\phi P_\lambda^{\mu-1}(\cos\theta)$$

$$\sigma_{yy} = 0$$

$$\sigma_{yz} = +\tfrac{1}{4}(-\lambda-\mu-2)_0 r^\lambda \sin(\mu+2)\phi P_\lambda^{\mu+2}(\cos\theta) - \tfrac{1}{4}(-\lambda-\mu-2)_4 r^\lambda \sin(\mu-2)\phi P_\lambda^{\mu-2}(\cos\theta)$$

Table 2. Solution B, $\mu = -1, -2, -3, \ldots$

$$\sigma_{yx} = -\tfrac{1}{2}\nu(-\lambda-\mu-2)_1 r^\lambda \sin(\mu+1)\phi P_\lambda^{\mu+1}(\cos\theta) + \tfrac{1}{2}\nu(-\lambda-\mu-2)_3 r^\lambda \sin(\mu-1)\phi P_\lambda^{\mu-1}(\cos\theta) + \tfrac{1}{4}(-\lambda-\mu-2)_1 r^\lambda \cos(\mu+2)\phi \sin\phi \sin\theta P_{\lambda-1}^{\mu+2}(\cos\theta) - \tfrac{1}{4}(-\lambda-\mu-2)_5 r^\lambda \cos(\mu-2)\phi \sin\phi \sin\theta P_{\lambda-1}^{\mu-2}(\cos\theta)$$

$$\sigma_{yy} = \tfrac{1}{4}(-\lambda-\mu-2)_1 r^\lambda \sin(\mu+2)\phi \sin\phi \sin\theta P_{\lambda-1}^{\mu+2}(\cos\theta) + \tfrac{1}{4}(-\lambda-\mu-2)_5 r^\lambda \sin(\mu-2)\phi \sin\phi \sin\theta P_{\lambda-1}^{\mu-2}(\cos\theta) + \tfrac{1}{2}(-\lambda-\mu-2)_3 r^\lambda \sin\mu\phi \sin\phi \sin\theta P_{\lambda-1}^{\mu}(\cos\theta)$$

$$\sigma_{yz} = \left(\tfrac{1}{2}+\frac{\nu}{2}\right)(-\lambda-\mu-2)_2 r^\lambda \sin\mu\phi P_\lambda^\mu(\cos\theta) + \tfrac{1}{4}(1-\nu)(-\lambda-\mu-2)_0 r^\lambda \sin(\mu+2)\phi P_\lambda^{\mu+2}(\cos\theta) + \tfrac{1}{4}(1-\nu)(-\lambda-\mu-2)_4 r^\lambda \sin(\mu-2)\phi P_\lambda^{\mu-2}(\cos\theta) - \tfrac{1}{2}(-\lambda-\mu-2)_2 r^\lambda \cos(\mu+1)\phi \sin\phi \sin\theta P_{\lambda-1}^{\mu+1}(\cos\theta) - \tfrac{1}{2}(-\lambda-\mu-2)_4 r^\lambda \cos(\mu-1)\phi \sin\phi \sin\theta P_{\lambda-1}^{\mu-1}(\cos\theta)$$

Table 3. Solution C, $\mu = -\frac{3}{2}, -\frac{5}{2}, -\frac{7}{2}, \ldots$

$$\sigma_{yx} = -\tfrac{1}{8}(-\lambda-\mu-2)_0 r^\lambda \sin(\mu+3)\phi \sin\phi \sin\theta P_{\lambda-1}^{\mu+3}(\cos\theta) + \tfrac{1}{8}(-\lambda-\mu-2)_6 r^\lambda \sin(\mu-3)\phi \sin\phi \sin\theta P_{\lambda-1}^{\mu-3}(\cos\theta) - \tfrac{1}{8}(-\lambda-\mu-2)_2 r^\lambda \sin(\mu+1)\phi \sin\phi \sin\theta P_{\lambda-1}^{\mu+1}(\cos\theta) + \tfrac{1}{8}(-\lambda-\mu-2)_4 r^\lambda \sin(\mu-1)\phi \sin\phi \sin\theta P_{\lambda-1}^{\mu-1}(\cos\theta)$$

$$\sigma_{yy} = \tfrac{1}{4}(-\lambda-\mu-2)_0 r^\lambda \sin(\mu+2)\phi P_\lambda^{\mu+2}(\cos\theta) + \tfrac{1}{4}(-\lambda-\mu-2)_4 r^\lambda \sin(\mu-2)\phi P_\lambda^{\mu-2}(\cos\theta) + \tfrac{1}{2}(-\lambda-\mu-2)_2 r^\lambda \sin\mu\phi P_\lambda^\mu(\cos\theta) + \tfrac{1}{8}(-\lambda-\mu-2)_0 r^\lambda \cos(\mu+3)\phi \sin\phi \sin\theta P_{\lambda-1}^{\mu+3}(\cos\theta) + \tfrac{1}{8}(-\lambda-\mu-2)_6 r^\lambda \cos(\mu-3)\phi \sin\phi \sin\theta P_{\lambda-1}^{\mu-3}(\cos\theta) + \tfrac{3}{8}(-\lambda-\mu-2)_2 r^\lambda \cos(\mu+1)\phi \sin\phi \sin\theta P_{\lambda-1}^{\mu+1}(\cos\theta) + \tfrac{3}{8}(-\lambda-\mu-2)_4 r^\lambda \cos(\mu-1)\phi \sin\phi \sin\theta P_{\lambda-1}^{\mu-1}(\cos\theta)$$

$$\sigma_{yz} = \tfrac{1}{4}(-\lambda-\mu-2)_1 r^\lambda \sin(\mu+2)\phi \sin\phi \sin\theta P_{\lambda-1}^{\mu+2}(\cos\theta) + \tfrac{1}{4}(-\lambda-\mu-2)_5 r^\lambda \sin(\mu-2)\phi \sin\phi \sin\theta P_{\lambda-1}^{\mu-2}(\cos\theta) + \tfrac{1}{2}(-\lambda-\mu-2)_3 r^\lambda \sin\mu\phi \sin\phi \sin\theta P_{\lambda-1}^{\mu}(\cos\theta)$$

may replace solution C by the simpler one

$$\text{sol. } 6\,\{\psi_6 = r^{\lambda+1}\cos\mu\phi P_{\lambda+1}^{\mu}(\cos\theta)/G\},$$
$$\mu = -\tfrac{1}{2}, -\tfrac{3}{2}, -\tfrac{5}{2}, \ldots \tag{4.4}$$

from which the special case $\mu = -\frac{1}{2}$ is independent of soliutions A, B and C.

5. AN INEFFECTIVE NEXT STEP

It seems probable that some more investigators have tried to create solutions like our solutions A, B and C. It will have occured to them, that among such solutions, whatever λ values are taken, there is no one which obeys the conditions $\sigma_{zx} = 0$, $\sigma_{zy} = 0$, $\sigma_{zz} = 0$ at the half-space surface, apart from trivial cases (such cases are two rigid body translations and a rotation, a constant stress σ_{xx}, a stress $\sigma_{xx} = z$, a stress $\sigma_{xx} = -x$ together with $\sigma_{xy} = y$, a stress $\sigma_{xx} = -x$ together with $\sigma_{xz} = z$, the three combined stresses $\sigma_{xx} = -2(1+\nu)xz$, $\sigma_{xy} = 2\nu yz$, $\sigma_{xz} = z^2$, cases of plane strain for Poisson's ratio $\nu = 0$). Neither is there a combination of a small number of such solutions which attains the contemplated effect.

It looks plausible, however, to suppose that an infinite number of such solutions in the proper combination, may fit, for special λ values, the conditions of $\sigma_{zx} = 0$, $\sigma_{zy} = 0$, $\sigma_{zz} = 0$ at the half-space surface.

In such a combination of an infinite number of solutions A, B and C we assign $3 \times \infty$ unknown participation factors to these solutions. Consider then the expressions for σ_{zx}, σ_{zy} and σ_{zz} (at $\theta = \pi/2$) separately.

Apply the operator

$$\left.\begin{array}{l} \text{on } \sigma_{zx}, \int_0^{2\pi} \ldots \cos(n-1)\phi d\phi \\ \text{on } \sigma_{zy}, \int_0^{2\pi} \ldots \sin n\phi d\phi \\ \text{on } \sigma_{zz}, \int_0^{2\pi} \ldots \cos(n-1)\phi d\phi \end{array}\right\} n = 1, 2, 3 \ldots \tag{5.1}$$

and get an infinite set of equations with zero right-hand sides. From the condition that the determinant of this set be zero the value of λ with minimum $Re\,\lambda > -\frac{3}{2}$ must be solved.

The determinant must of course be truncated. Though there are computerprograms to calculate the value of determinants, a determinant of high order, without special scaling, very often has an absolute value too large or too small for the computer, which always has limitations for the exponents of powers of 10 (for the computer used +76 and −76). Besides, without further special scaling, the value of a determinant of infinite order does not converge when successive truncations are being tried . Therefore a method is applied, which we have called the "resonance" method.

The half-space surface ($z = 0$) was "struck" by an arbitrary load

$$\begin{aligned} \sigma_{zx} &= 0 \\ \sigma_{zy} &= 0 \\ \sigma_{zz} &= r^{\lambda}\dagger \end{aligned} \tag{5.2}$$

and the combination of the infinite number of solutions A, B and C with their unknown participation factors is sought which corresponds to the load (5.2). Application of the operators (5.1) gives again the same equations, but now the right hand members are not all zero.

A sequence of λ values is tried and the response of the participation factors is studied. The value of λ for which one, some, or all participation factors become infinite represents an eigenvalue λ. One should compare this phenomenon with the striking of an elastic structure by prescribed forces in one of the eigenfrequencies ω of the structure. In stead of ω (in exp $i\omega t$) the exponent λ (in r^{λ}) plays the rôle of an "eigenfrequency" (ω is always real, λ may be complex). To detect such a λ value, the reciprocal of a dominant participation factor, for example that of sol. C, $\mu = -\frac{3}{2}$, is plotted vs the λ values tried and the root-value λ is detected with sufficient accuracy. The participation factors, tending to infinity, preserve their mutual ratios. The combined stress-systems, multiplied by these participation factors, form together an eigenfunction for the stresses. It is true that this eigenfunction, tending to infinity, still produces the load, but this load becomes, relatively, infinitely small.

In designing this procedure, it was assumed that the solutions A, B and C with the proper μ values form a complete set to meet an arbitrary load, like (5.2) at the half-space surface, but of course with exception for the roots λ, that are to be found.

There is a good reason for this assumption because there are no other solutions separated into variables, which obey the boundary conditions at the crack (at arbitrary values of λ) than the ones used with their proper μ values. It is however a disturbing fact that for the solution C the value $\mu = -\frac{1}{2}$ is forbidden (then there would be a $\theta^{-3/2}$ singularity along the z-axis). Likewise, it is a disturbing fact that in the case of an incompressible medium ($\nu = \frac{1}{2}$), the solution C may be replaced by the simpler solution (4.4), which practically means that one has one additional degree of freedom to meet the prescribed load (sol. 6, $\mu = -\frac{1}{2}$).

Nevertheless, it was hoped, that the set (4.3) would be complete in the sense that was needed for the devised procedure. The numerical results decisively showed it was not. The calculated stresses in the interior did not converge at successive truncations and did not fit the prescribed load (5.2) at all. For these stresses at the half-space surface heavily oscillating functions of order 10 (at $r = 1$) were found in stead of $\sigma_{zx} = 0$, $\sigma_{zy} = 0$, $\sigma_{zz} = 1$.

†Some final results were checked by starting with $\sigma_{zx} = r^{\lambda}$, $\sigma_{zy} = 0$, $\sigma_{zz} = 0$ and $\sigma_{zx} = 0$, $\sigma_{zy} = r^{\lambda} \sin\phi$, $\sigma_{zz} = 0$.

Introduction of the $\mu = -\frac{1}{2}$ value in the solution C (though forbidden) or use of solution (4.4) in the case of the incompressible medium did not much improve the situation. This suggests that more than one degree of freedom for the stresses in the set (4.3) is lacking to meet the conditions of (5.2), in spite of the fact that already $3 \times \infty$ degrees of freedom were used.

6. CREATION OF SOME ADDITIONAL DEGREES OF FREEDOM

Tentatively 4 more degrees of freedom were added. They are derived from the solutions D and E. In contrast to the $3 \times \infty$ degrees of freedom from the solutions A, B and C the solutions D and E do not yet leave the crack surfaces stressfree.

$$\begin{aligned} \text{sol. } D = \text{sol. } 7 \{&\psi_7 = r^{\lambda+1} \cos \mu\phi P^{\mu}_{\lambda+1}(\cos\theta)/G \\ &+ (\lambda+\mu+1)(\lambda-\mu+2) r^{\lambda+1} \cos(\mu-2)\phi P^{\mu-2}_{\lambda+1}(\cos\theta)/G\} \\ &\mu = 0 \text{ and } -1 \end{aligned} \tag{6.1}$$

$$\begin{aligned} \text{sol. } E = \text{sol. } 7 \Big\{&\psi_7 = r^{\lambda+1} \sin \mu\phi P^{\mu}_{\lambda+1}(\cos\theta)/G \\ &+ \frac{\mu(\lambda+\mu+1)(\lambda-\mu+2)}{\mu-2} r^{\lambda+1} \sin(\mu-2)\phi P^{\mu-2}_{\lambda+1}(\cos\theta)/G\Big\} \\ &\mu = -\tfrac{3}{2} \text{ and } -\tfrac{5}{2}. \end{aligned} \tag{6.2}$$

The solutions D generally show at the crack-surfaces a normal stress σ_{yy}, the solutions E shear stresses σ_{yx} and σ_{yz}, but the structure of these solutions is choosen such that these unwanted stresses may be removed by the solutions a, b and c, skew-symmetrical to the plane $z = 0$, especially created for this purpose. The solutions D and E adjusted in this way will be called

$$\begin{aligned} &\text{sol. } D^* \ (\mu = 0 \text{ and } -1) \\ &\text{sol. } E^* \ (\mu = -\tfrac{3}{2} \text{ and } -\tfrac{5}{2}). \end{aligned} \tag{6.3}$$

It can be proved that the solutions a, b and c form a complete set to achieve the purpose at hand. They are defined with the aid of *another* spherical coordinate system with the polar axis along the y-axis.

$$\begin{aligned} x &= r \sin\beta \cos\alpha \\ y &= r \cos\beta \\ z &= r \sin\beta \sin\alpha. \end{aligned} \tag{6.4}$$

Again, the solutions a, b and c are derived from the solutions 1 . . . 7 of Section 3

$$\begin{aligned} \text{sol. } a = \text{sol. } 4 \{&\psi_4 = (1-2\nu)\psi_a\} + \text{sol. } 6 \ (\psi_6 = \partial\psi_a/\partial y) \\ &\psi_a = r^{\lambda+2} \sin \mu\alpha P^{\mu}_{\lambda+2}(\cos\beta)/G \\ &\mu = -1, -2, -3, \ldots \\ \text{sol. } b = \text{sol. } 2 \ (&\psi_2 = 2\psi_b) \\ &\psi_b = r^{\lambda+2} \cos \mu\alpha P^{\mu}_{\lambda+2}(\cos\beta)/G \\ &\mu = 0, -1, -2, \ldots \\ \text{sol. } c = \text{sol. } 4 \{&\psi_4 = 2(1-\nu)\psi_c\} + \text{sol. } 6 \ (\psi_6 = \partial\psi_c/\partial y) \\ &\psi_c = r^{\lambda+2} \sin \mu\alpha P^{\mu}_{\lambda+2}(\cos\beta)/G \\ &\mu = -1, -2, -3, \ldots . \end{aligned} \tag{6.5}$$

Apart from being skew-symmetrical stress systems (with respect to $z = 0$), the solutions a have at $y = 0$, i.e. $\beta = \pi/2$ (thus also at the crack surfaces), zero shear stresses σ_{yx} and σ_{yz}. The solutions b and c have there a zero normal stress σ_{yy}.

To remove the unwanted stresses at the crack surfaces of solutions D and E, generally an infinite number of solutions a, b and c will be necessary. The infinite series of these solutions will be only convergent in the region $0 \leq \beta \leq \pi/2$ because of the fact that the $P_\lambda^\mu(\cos\beta)$ functions show a $(\pi-\beta)^\mu$ singularity along the negative y-axis ($\beta \to \pi$). The series will however be enforced to retain the conditions $v = 0$, $\sigma_{yx} = 0$, $\sigma_{yz} = 0$ in the plane of symmetry $\phi = \pi$. This guaranties that the stresses represented by these series have their symmetrical analytical continuation in the region $\beta > \pi/2$.

The participation factors of the different solutions b ($\mu = 0, -1, -2, \ldots$) and c ($\mu = -1, -2, \ldots$) follow from a generalized Fourier-analysis, those of solution a ($\mu = -1, -2, \ldots$) must follow from an (truncated) infinite set of equations.

The participation factors of the solutions a were however not choosen as the primary unknowns but coefficients B_m and C_m in

$$v = r^{\lambda+1} \sum_m B_m \cos m\alpha \sin\alpha (\cos\alpha)^{1/2} + \text{known part} \tag{6.6}$$

$$\sigma_{yy} = r^\lambda \sum_m C_m \cos m\xi \sin\xi (\cos\xi)^{-(1/2)} + \text{known part} \tag{6.7}$$

$$m = 0, 2, 4, \ldots, \quad \xi = \pi - \alpha.$$

In (6.6) the displacements v must become those of the solutions D^* and E^* of (6.3) at the crack plane $\phi = +0$. The angle α is from the coordinate system (6.4). The stresses σ_{yy} must be from these solutions in plane of symmetry $\phi = \pi$. When the unknowns B_m and C_m are once solved, also the participation factors for the solutions a, $\mu = -1, -2, -3, \ldots$ are easily found.

It is to be seen from (6.6), (6.7) that for the displacements v and the stresses σ_{yy} it is assumed that they, just as the plane strain solution and the solution C, $\mu = -\frac{3}{2}$, exhibit a singularity along the crack front in α. These singularities are of type $\theta^{1/2}$ and $\theta^{-(1/2)}$ ($\theta \to 0$) respectively.

These singularities become at $r = 1$

$$\begin{aligned} &\text{for } v \text{ in } \phi = 0 && v = (B_0 - B_2 + B_4 - \cdots)\theta^{1/2} \\ &\text{for } \sigma_{yy} \text{ in } \phi = \pi && \sigma_{yy} = (C_0 - C_2 + C_4 - \cdots)\theta^{-(1/2)}. \end{aligned} \tag{6.8}$$

The assumptions concerning these singularities were confirmed by the ratio of the "coefficients" of these singularities, viz.

$$\frac{B_0 - B_2 + B_4 - \cdots}{C_0 - C_2 + C_4 - \cdots} \tag{6.9}$$

which converged at successive truncations to $2(1-\nu)/G$, this being also the ratio for solution C, $\mu = -\frac{3}{2}$, plane strain included, $\lambda = -\frac{1}{2}$.

7. THE SOLUTION OF THE EQUATIONS AND DETERMINATION OF THE EIGENVALUES

Now the infinite number of
solutions A, $\mu = 0, -1, -2, \ldots$
solutions B, $\mu = -1, -2, -3, \ldots$
solutions C, $\mu = -\frac{3}{2}, -\frac{5}{2}, -\frac{7}{2}, \ldots$
solutions D^*, $\mu = 0$ and -1 only,
solutions E^*, $\mu = -\frac{3}{2}$ and $-\frac{5}{2}$ only,
is employed to meet the load (5.2).

The infinite set of equations for the participation factors are again obtained by application of the operators (5.1). As far as the (four) solutions D^* and E^* are concerned, some integrations had to be carried out numerically.

In the actual calculations, of course, not an infinite number of solutions A, B and C can be taken, but from each of them a number of 8 or 16 was used (occasionally also 12, 20 or 24). So the

number of "degrees of freedom" for the stresses was respectively $3\times 8+4=28$ and $3\times 16+4=52$ (occasionally 40, 64, 76). The prescribed load is well reproduced and also the stresses elsewhere in the half-space converge very well when the number of degrees of freedom is increased (28, 40, 52, 64, 76).

Different values of λ occurring in the exponent of (5.2) are tried and the reciprocal of a predominant unknown is plotted vs the varying λ and where the curve crosses the horizontal axis, the "resonance" value of λ is found.

Figure 2 gives the roots for λ as function of Poisson's ratio ν and Table 4 the numerical values.

In the plot of Fig. 2 the points A and B were known exactly beforehand. They represent two cases of plane strain for Poisson's ratio $\nu = 0$. Both the eigenfunctions for the stresses are sol. C, $\mu = -\frac{3}{2}$ and $-\frac{5}{2}$ respectively.

Next to the curve, one could indicate in Fig. 2 three more lines. They represent also solutions of the Navier–Cauchy equations which obey the crack-surfaces and half-space surface stress-free conditions. These lines are: (1) a double line at $\lambda = -1$, representing two rigid body translations u = constant and w = constant; (2) a double line at $\lambda = 0$ representing a rigid body rotation around the y-axis and a constant stress σ_{xx}; (3) a triple line at $\lambda = 1$ representing the case $\sigma_{xx} = z$, the case $\sigma_{xx} = -x$ together with $\sigma_{xy} = y$ and the case $\sigma_{xx} = -x$ together with $\sigma_{xz} = z$.

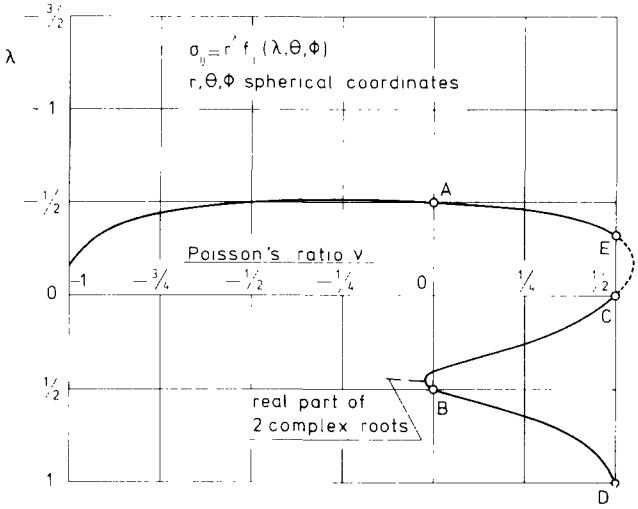

Fig. 2. Exponents of the three-dimensional stress-singularities of the quarter-infinite crack in the half-space. A, B, C, D exact points. E experimental verification.

Table 4. Computed λ values in $\sigma_{ij} = r^{\lambda} f_{ij}(\lambda, \theta, \phi)$

Poisson's ratio ν	λ
0.0	−0.5
0.15	−0.4836
0.3	−0.4523
0.4	−0.4132
0.5	−0.3318
0.5	0.0
0.4	0.135
0.3	0.218
0.15	0.309
0.075	0.355
0.0	0.410
0.0	0.5
0.075	0.553
0.15	0.594
0.3	0.681
0.4	0.765
0.475	0.898
0.5	1.0

The rigid body rotation around the y-axis is represented, for all Poisson's ratios, by $(1-\nu)$ sol. A $(\lambda=0,\ \mu=0)+12$ sol. B $(\lambda=0,\ \mu=-2)$ which combination of solutions gives $Gu=-2(1-\nu)z$, $Gw=2(1-\nu)x$. There is however, another solution which gives a rigid body rotation around the y-axis, but only for Poisson's ratio $\nu=\frac{1}{2}$. This solution is sol. D^* $(\lambda=0,\ \mu=-1)=$ sol. D and it gives $Gu=\frac{1}{2}z$, $Gw=-\frac{1}{2}x$. The occurence of this extra "rigid-body-rotation-solution" is the reason why the curve crosses the line $\lambda=0$ exactly in the point $\nu=\frac{1}{2}$ (point C).

The solution $\sigma_{xx}=z$ is represented, for all Poisson's ratios, by sol. B $(\lambda=1,\ \mu=-1)-$ sol. A $(\lambda=1,\ \mu=-1)-(12+2\nu)$ sol. A $(\lambda=1,\ \mu=-3)$. In fact this combination gives $\sigma_{xx}=(2\nu+2)z$. There is another combination, but only for Poisson's ratio $\nu=\frac{1}{2}$, which gives the same stress. It is sol. $D(\lambda=1,\ \mu=0)-18$ sol. D $(\lambda=1,\ \mu=-2)$ which gives $\sigma_{xx}=-12z$. The occurence of this "extra solution $\sigma_{xx}=z$" is the reason why the curve crosses the line $\lambda=1$ exactly in the point $\nu=\frac{1}{2}$ (point D).

8. THE EIGENFUNCTIONS FOR THE STRESSES AND DISPLACEMENTS. THE STRESS-INTENSITY FACTOR

To each eigenvalue λ belongs an eigenfunction for the stresses and displacements. For the gravest value of λ the non-zero stresses at the half-space surface $(z=0)$ are given for Poisson's ratio $\nu=\frac{1}{2}$ and $\nu=0.3$ in Figs. 3 and 4 as well as the displacements for $\nu=\frac{1}{2}$ in Fig. 5.

The stresses and displacements were normalized such that at the crackfront at $z=1$ (Fig. 1) the stress intensity factor $k=\sqrt{2}$. This means that in the plane $z=1$ the stress σ_{yy} behaves along

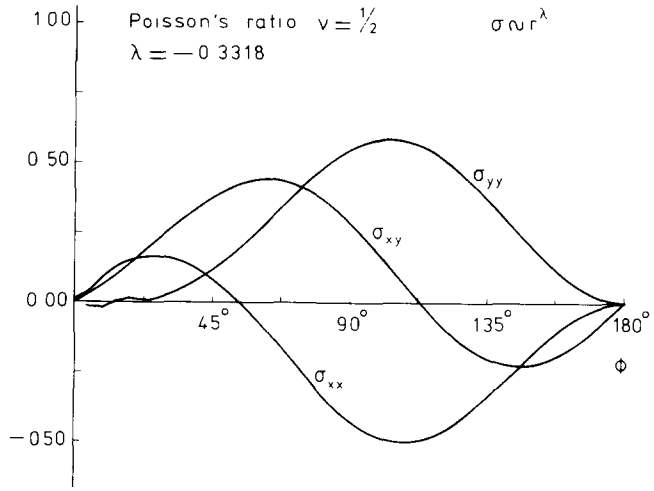

Fig. 3. Stresses at $z=0$, $r=1$. Stress-intensity factor at crack front at $z=1$ is $\sqrt{2}$. Poisson's ratio $\nu=\frac{1}{2}$.

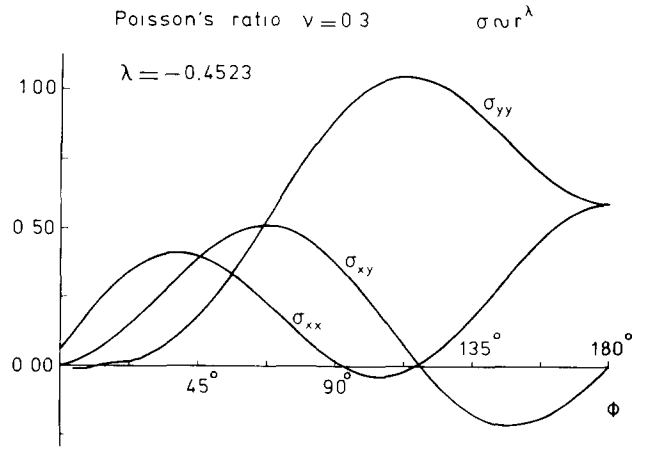

Fig. 4. Stresses at $z=0$, $r=1$. Stress-intensity factor at crack front at $z=1$ is $\sqrt{2}$. Poisson's ratio $\nu=0.3$.

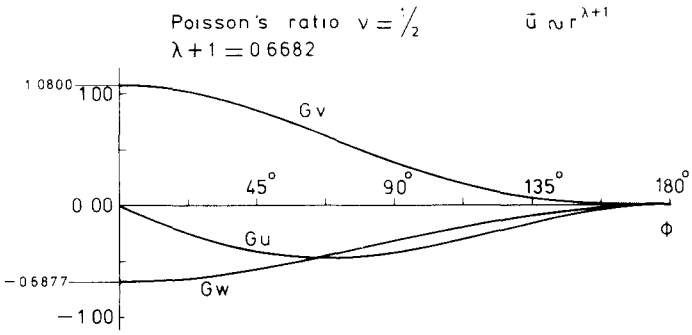

Fig. 5. Cartesian displacement components at $z = 0$, $r = 1$. Stress-intensity factor at crack front at $z = 1$ is $\sqrt{2}$. Poisson's ratio $\nu = \frac{1}{2}$.

the line $\phi = \pi$ (the elongation of the crack) as

$$\sigma_{yy} = \frac{k}{\sqrt{(2\rho)}} = \frac{1}{\sqrt{\rho}}, \quad \rho \to 0,\dagger \tag{8.1}$$

In (8.1) is ρ the distance to the crack tip (i.e. the radius of a cylindrical coordinate-system around the z-axis). We may also write for (8.1)

$$\sigma_{yy} = \frac{1}{\sqrt{\theta}}, \quad \theta \to 0 \ (z = 1, \phi = \pi). \tag{8.2}$$

Since the stresses behave (along all lines through the vertex) as

$$\sigma_{xx} = r^{\lambda} f_{xx}(\lambda, \theta, \phi); \quad \sigma_{xy} = r^{\lambda} f_{xy}(\lambda, \theta, \phi), \ldots,$$

the formula (8.2) for other planes z = constant becomes

$$\sigma_{yy} = z^{\lambda} \frac{1}{\sqrt{\theta}}, \quad \theta \to 0, \quad \phi = \pi$$

$$\sigma_{yy} = z^{\lambda + (1/2)} \frac{1}{\sqrt{\rho}}, \quad \rho \to 0, \quad \phi = \pi,$$

or with the aid of the stress-intensity factor k

$$\sigma_{yy} = \frac{k}{\sqrt{(2\rho)}}, \quad \rho \to 0, \quad \phi = \pi,$$

$$k = \sqrt{(2)} z^{\lambda + (1/2)}. \tag{8.3}$$

Hence at the half-space surface ($z = 0$) the stress-intensity factor is zero (if $\lambda > -\frac{1}{2}$). This does only mean that in the plane $z = 0$ there are no stresses that vary according to $\rho^{-(1/2)}$. Only a (somewhat) weaker exponent occurs. Indeed all stresses behave in that plane according to ρ^{λ} and they still tend to infinity for $\rho \to 0$. This clearly demonstrates that the two-dimensional conception of the stress-intensity factor looses its meaning in the vertex- region which is essentially three-dimensional.

Because the stresses σ_{zx}, σ_{zy}, σ_{zz} are zero at the half-space surface it is often said that the state of stress there is a state of "plane stress". However, the non-zero stresses do not obey the usual partial differential equations of two-dimensional elasticity theory. The exponent of the stress singularity around the crack is not the familiar $-\frac{1}{2}$ but λ, though admittedly the true exponent deviates only a little from $-\frac{1}{2}$. It is the more remarkable that the stresses are very significant for the Poisson's ratios for which they are plotted.

†Some authors define a stress-intensity factor which differs a factor $\sqrt{\pi}$ from the one used here.

Some further observations, considering the Figs. 3–5 can be made. (1) The stress σ_{yy} starts from $\phi = 0$ irregularly. This is not surprising. For $\phi \to 0$ holds

$$\sigma_{yy} = c\phi^{1.7396+1.1190i} + \bar{c}\phi^{1.7396-1.1190i}, \quad (\nu \neq 0).$$

The complex exponent is the gravest exponent from (2.2) with $\alpha = \pi/2$ of the free-free 90° wedge in plane strain. (2) At $\phi = \pi$ and $\nu = \frac{1}{2}$ (incompressible medium), Fig. 3, the stresses σ_{xx} and σ_{yy} are practically zero. (3) At $\phi = \pi$ and $\nu = \frac{1}{2}$ (incompressible medium) Fig. 5 gives with high accuracy $u = 0$, $w = 0$.

The observations (2) and (3) appear to be exactly true (see Appendix A).

9. EXPERIMENTAL VERIFICATION

Rubber is a material with a compression modulus some orders greater than the shear modulus, the reason why Poisson's ratio is practically $\frac{1}{2}$. It is a material in which an artificial crack with a sharp crack front is easily made by incision. Besides, rubber allows in many circumstances to apply larger displacements than metals do in experiments to test elasticity theory.

A symmetrical block of rubber, dimensions $40 \times 40 \times 40$ cm, was taken. Half-way an incision was made. Figure 6 shows the block in a position where it is loaded smoothly in some symmetrical way.

Both intersections of the crack surfaces with the upper surface of the loaded rubber block assume a curved shape. On the photograph Fig. 7 these both intersections are projected on a plane through the crack front and normal to the upper surface of the rubber block. To this purpose this photograph was taken in the plane of the upper surface of the block and in crack direction.

On the photograph Fig. 7 the projections of both intersections (of crack surfaces with upper surface) start at the vertex with a mutual angle, which theoretically must be 115.0. This angle is derived from the ordinates at $\phi = 0$ in Fig. 5,

$$180° - 2 \arctan \frac{0.6877}{1.0800} = 115.0°.$$

This angle is drawn in Fig. 7 and indeed the agreement is quite satisfactory. The angle is significant for Poisson's ratio $\nu = \frac{1}{2}$ and the exponent of the displacements ($r^{0.6682}$). The possibility to measure this angle in an easy way, was an excellent opportunity to get essential information on the surface displacements around the crack tip, without the necessity to measure the exponent of the displacement itself.

The significance of the angle of 115° for Poisson's ratio $\nu = \frac{1}{2}$ is further demonstrated by drawing the same angle for Poisson's ratio $\nu = 0.3$ being 138°.

Some further experimental verification may be found in Ref. [2].

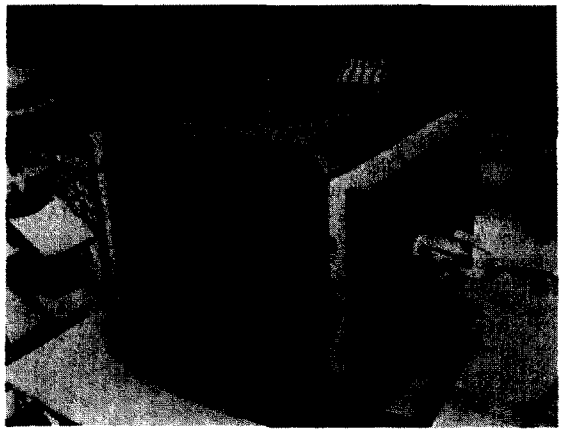

Fig. 6. The rubber block with incision (the artificial crack) in loaded position. Dimensions $40 \times 40 \times 40$ cm. The arrow indicates the line of sight into the crack opening of Fig. 7.

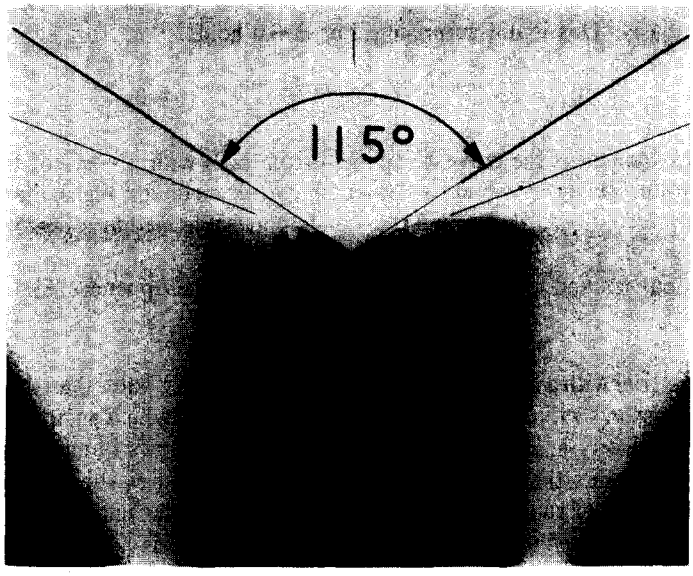

Fig. 7. Photograph into the crack opening of the loaded rubber block along the line of sight as indicated with the arrow in Fig. 6. The intersections of the crack planes with the upper surface of the rubber block become curved lines. As projected in the photograph both curved lines start at the crack front with a mutual angle, which theoretically must be 115° (Poisson's ratio $\nu = \frac{1}{2}$). For comparison also a wider angle of 138°, being the theoretical angle for Poisson's ratio $\nu = 0.3$, is indicated.

REFERENCES

1. G. C. Sih, A review of the three-dimensional stress problem for a cracked plate. *Int. J. Fract. Mech.* **7**, 39 (1971).
2. J. P. Benthem, Three-dimensional state of stress at the vertex of a quarter-infinite crack in a half-space. *Report WTHD Nr.* 74. Department of Mechanical Engineering, Delft University of Technology (September 1975).
3. M. L. Williams, Stress singularities resulting from various boundary conditions in angular corners of plates in extension. *J. Appl. Mech.* **19**, 526 (1952).
4. Z. P. Bažant, Three-dimensional harmonic functions near termination or intersection of gradient singularity lines: a general numerical method. *Int. J. Engng. Sci.* **12**, 221–243 (1974).
5. H. M. Westergaard, Effects of a change of Poison's ratio analyzed by twinned gradients. *J. Appl. Mech.* **7**, A 113 (1940).

APPENDIX A

Some peculiarities of the eigenfunctions of the incompressible medium

Some peculiarities of the eigenfunctions for the displacements and the stresses of the incompressible medium ($\nu = \frac{1}{2}$) were observed. They are that at the half-space surface at the lengthening of the crack the displacements u and w are zero and that the stresses σ_{xx} and σ_{yy} are zero.

Only after the numerical establishment of these facts it was realised that these observations are exactly true.

To make this plausible, we start with the Kelvin-solution for the concentrated force acting on the surface of a semi-infinite incompressible medium (see for example Ref. [5]). From this solution is learned that forces in x, y and z-direction in the origin of the half-space $z > 0$, leave the plane $y = 0$ stress-free, i.e. $\sigma_{yx} = \sigma_{yy} = \sigma_{yz} = 0$. By differentiation of the Kelvin-solution it follows that a double-force acting at the origin in y-direction also leaves the plane $y = 0$ stress-free.

The reciprocal theorem of elasticity theory now learns that if on the crack-surfaces a normal load is applied (in a symmetrical way) there will be no displacements u and w along $z = 0$, $y = 0$ and no strains ϵ_{xx} and ϵ_{yy}. Thus at the half-space surface at the lengthening of the crack, next to $\sigma_{zz} = \sigma_{zx} = \sigma_{zy} = \sigma_{xy} = 0$ and $v = 0$, it is found

$$u = 0, \quad w = 0, \quad \sigma_{xx} = 0, \quad \sigma_{yy} = 0. \tag{A1}$$

The eigenfunctions for the stresses have been, however, not generated with the resonance-method by normal loading of the crack surfaces, but by normal loading of the half-space surface. This could however, though with less numerical efficiency, equally have been done by normal loading of the crack surfaces. The responding stresses, tending to infinity at resonance, would remain showing the peculiarities (A1). The numerical establishment of (A1) is considered to be a fair check on the rightness of the calculations, also in the case of $\nu \neq \frac{1}{2}$.

There are some trivial eigenfunctions which cannot be raised by resonance through normal loading of the crack surfaces (because they exhibit a stress $\sigma_{yy} = 0$ in all space) and indeed they do not show all the peculiarities (A1). Such eigenfunctions are (also valid for $\nu \neq \frac{1}{2}$) some of the trival cases mentioned in Section 5, for example for rigid-body displacement w = constant.